A Molecular Dynamics Exploration of the Catalytic Mechanism of Yeast Cytosine Deaminase

Lishan Yao,[†,§] Stepan Sklenak,[§] Honggao Yan,*[,‡,§] and Robert I. Cukier*[,†,§]

Department of Chemistry, Department of Biochemistry and Molecular Biology, MSU Center for Biological Modeling, Michigan State University, East Lansing, Michigan 48824

Received: November 11, 2004; In Final Form: February 3, 2005

Yeast cytosine deaminase (yCD), a zinc metalloenzyme of significant biomedical interest, is investigated by a series of molecular dynamics simulations in its free form and complexed with its reactant (cytosine), product (uracil), several reaction intermediates, and an intermediate analogue. Quantum chemical calculations, used to construct a model for the catalytic Zn ion with its ligands (two cysteines, a histidine, and one water) show, by comparison with crystal structure data, that the cysteines are deprotonated and the histidine is monoprotonated. The simulations suggest that Glu64 plays a critical role in the catalysis by yCD. The rotation of the Glu64 side-chain carboxyl group that can be protonated or deprotonated permits it to act as a proton shuttle between the Zn-bound water and cytosine and subsequent reaction intermediates. Free energy methods are used to obtain the barriers for these rotations, and they are sufficiently small to permit rotation on a nanosecond time scale. In the course of the reaction, cytosine reorients to a geometry to favor nucleophilic attack by a Zn-bound hydroxide. A stable position for a reaction product, ammonia, was located in the active site, and the free energy of exchange with a water molecule was evaluated. The simulations also reveal small motions of the C-terminus and the loop that contains Phe114 that may be important for reactant binding and product release.

I. Introduction

Yeast cytosine deaminase (yCD) catalyzes the deamination of cytosine to uracil by nucleophilic attack of a Zn-bound hydroxide on the substrate, forming a tetrahedral intermediate that decomposes through the elimination of ammonia. Cytosine deaminase is present in bacteria and fungi, as part of the pyrimidine salvage pathway, but is absent in mammals.[1] yCD can also catalyze the deamination of the prodrug 5-fluorocytosine (5-FC) to the anticancer drug 5-fluorouracil (5-FU). Therefore, a potential system for gene-directed enzyme prodrug therapy combines yCD and the prodrug 5-FC, because the product, 5-FU, inhibits DNA synthesis and is thus a potent chemotherapeutic agent.[2,3]

High-resolution structures of yCD in the apo form[4] and in complex with the inhibitor 2-pyrimidinone, a mimic of a reaction intermediate,[4,5] are available. yCD is a homodimer, with each 158-residue subunit consisting of a central β-sheet flanked by two α-helices on one side and three α-helices on the other (Figure 1a). A single active site is present in each subunit. The active sites are separated by 14 Å, both are adjacent to the dimer interface, and no cooperativity has been reported for the enzyme.[4] Each active center contains a single catalytic zinc ion that is tetrahedrally coordinated by a histidine (His62), two cysteines (Cys91 and Cys94), and a water molecule in the substrate-free enzyme or the inhibitor in the complex (Figure 1b). The bound inhibitor is completely buried by a lid composed of Phe114 from the loop between β4 and α4 and Trp152 and Ile156, both from the C-terminal helix. Surprisingly, the structure of apo yCD is essentially the same as that of the intermediate analogue complex with a root-mean-squared deviation (RMSD) between the two structures of 0.23 Å for the backbone atoms.

The active site architectures of yCD and cytidine deaminase (CDA) from *E. coli* share a striking similarity.[6,7] Superposition of their active sites reveals a very similar interaction network involving the ligated water molecule, the Zn ion ligated by two cysteine residues and one histidine, the Zn-bound ligand, and a glutamic acid important to the catalytic mechanism.[5] On the basis of the similarity of these active site structures and early studies of the mechanism of CDA catalysis, an analogous reaction mechanism was proposed for yCD.[5] Our recent quantum chemical study[8] using the ONIOM(B3LYP:PM3) method has revealed a complete path for the deamination reaction catalyzed by yCD. The cytosine deamination proceeds via a sequential mechanism involving the protonation of N3, the nucleophilic attack of C4 by the Zn-coordinated hydroxide, and the cleavage of the C4−N4 bond. Uracil is liberated from the zinc by an oxygen exchange mechanism that involves the formation of a gem-diol intermediate from the Zn-bound uracil and a water molecule, $C4-O^{Zn}$ bond cleavage, and regeneration of the Zn-coordinated water.

In this article, we explore aspects of the mechanism of the cytosine deamination reaction by running a series of molecular dynamics (MD) trajectories (∼2 ns) for the fully solvated enzyme in its free form, reactant complex form, product complex form, and four possible intermediate complex forms, with active site structures summarized in Figure 2. In particular, we study the side-chain motion of Glu64 along the proposed[8] reaction path and the role of several other residues in both ligand binding and catalysis. For each simulation, quantum chemical calcula-

* Corresponding authors. Phone 517-355-9715 x 263, fax 517-353-1793, e-mail cukier@cem.msu.edu (R.L.C.). Phone 517-353-5282, fax 517-353-9334, e-mail yanh@msu.edu (H.Y.).
† Department of Chemistry.
‡ Department of Biochemistry and Molecular Biology.
§ MSU Center for Biological Modeling.

10.1021/jp044828+ CCC: $30.25
Published on Web 03/17/2005

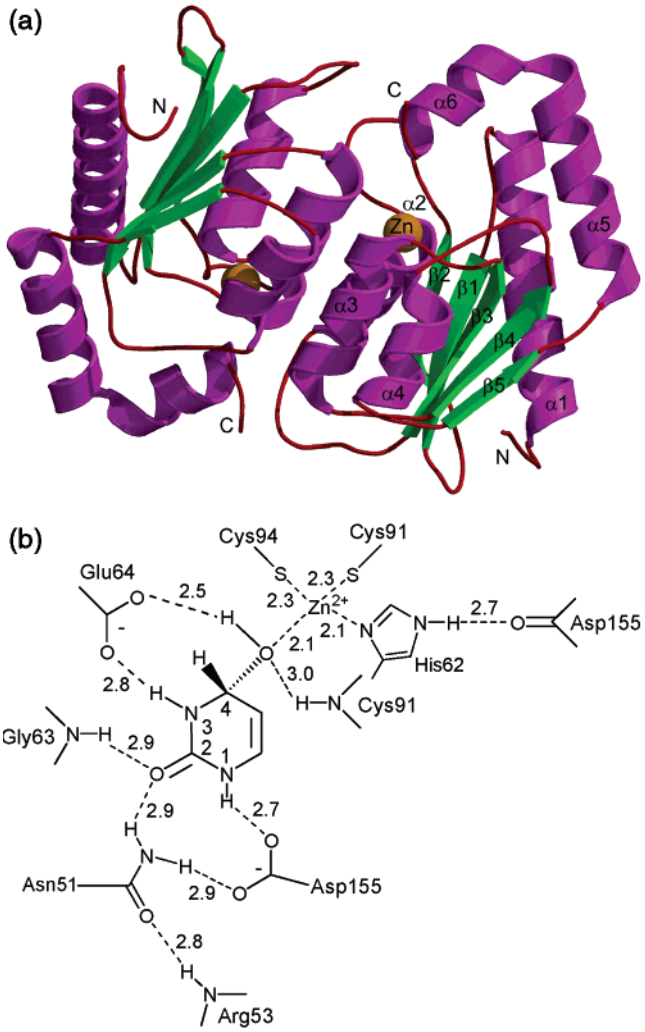

Figure 1. (a) Ribbon representation of the crystal structure of yCD drawn according to the coordinate of the 1.14-Å crystal structure.[4] α-Helices are colored magenta and *β*-strands green. N- and C-termini are labeled for both subunits of the homodimeric protein, and secondary structure elements are labeled for the subunit on the right only. The protein contains two active centers, with each active center composed of residues within a single subunit and a catalytic zinc ion (orange ball). The figure was prepared with Molscript[26] and Raster3D.[27,28] (b) Schematic drawing of the coordination sphere of the catalytic zinc ion and polar interactions between yCD and a reaction intermediate analogue as revealed by X-ray crystallography.[4,5] The distances (Å) between the zinc ion and its ligands and between the heavy atoms involved in hydrogen bonds are obtained from one subunit (A) of the 1.14-Å crystal structure of yCD with the reaction intermediate analogue complex. The distances vary slightly between subunits and between the two crystal structures of the yCD reaction intermediate analogue complex.[4,5]

tions are first carried out in order to obtain suitable charge parameters for the Zn ion, ligated residues, catalytic water, substrate, and important neighboring residues. The protonation states of the Zn-ligated residues are critical for an accurate simulation, as is an account of the substantial charge transfer to the Zn (formally 2+) ion. The availability of the yCD crystal structures with the intermediate analogue complex[4,5] aided us in validating the charge parameters of the Zn-bound complex by comparing the results of an MD simulation with these crystal structures.

The flexibility and average position of the loop containing Phe114 and the N- and C-terminal helices are monitored in the MD simulations of both the free and the intermediate analogue complex forms and compared with the corresponding crystal structures. That permits suggestions for possible ways the reaction products can exit the active site, of interest in view of the very similar crystal structures found for the apo and inhibitor-bound structures. The product complex simulation also suggests a binding position for ammonia and the exchanged water prior to release from the active site. In these ways, further insights into the catalytic and binding events taking place in the active site of yCD can be obtained.

II. Methods

Determination of the Protonation State of the Zn-Bound Complex. The protonation states of the Zn ligands, cysteine and histidine, are dependent on their surroundings.[9−11] Quantum chemical studies on model compounds show that the Zn−ligand distances are sensitive to their protonation states, and by comparison with crystallographic data, the latter can be reliably assigned.[9,10] We carried out B3LYP/6-31G** optimizations[8] in the gas phase for the Zn complexes starting from the crystal structure, modeling His62 by imidazole, Cys91 and Cys94 by −SCH3, and Glu64 by CH3CH2COO−, and included the Zn ion, a water, and −OOCCH2CH2C(═O)CH3, the last of which is a model for Asp155 that is hydrogen-bonded to His62 (2.7 Å, a second-shell interaction with Zn) and, in the intermediate analogue complex, also to the intermediate analogue (Figure 1b). These calculations showed that, to match the coordination geometry of the zinc ion in the crystal structure, the sulfur atoms of Cys91 and Cys94 must be deprotonated, and His62 must be singly protonated.

Parameterization of the Zn-Bound Complex. In metal-ligated simulations, a choice between bonded versus nonbonded force fields must be made.[12] For the purposes of this work, where the crystal structures show strong four-coordinate ligation to the Zn ion, a bonded (covalent) force field is indicated. Thus, explicit bonds between the Zn cation and its ligands were used.[13] The force constants for bonds and bond angles listed in Table 1 serve to preserve the experimentally observed tetrahedral Zn. They are consistent with force constants used for a Zn complex in a recent simulation by Suarez and Merz.[14] The equilibrium bond distances and angles are taken from the apo yCD crystal structure.[4] All the torsional parameters associated with the Zn−ligand interactions were set to zero as in Hoops et al.[13]

A single-point quantum mechanics (QM) calculation (B3LYP/6-31+G*) of the Zn complex was carried out on the basis of the crystal structure of the yCD free form. Zn, its three ligated residues, His62, Cys91, and Cys94, as well as Asp155 (all atoms), and one water molecule (coordinated with the Zn) are included in the calculation. Hydrogen atoms were added by using the Insight II program. One hydrogen atom was added to each C-terminus and N-terminus of the four amino acids to saturate the heavy atoms. Atom-centered partial charges were derived by using the AMBER antechamber program (RESP methodology).[15] Though HF/6-31G* is the method used for parameterization of the general AMBER force field (GAFF),[16] in the case of the Zn-ligand bonds that have an intermediate character between a covalent and an ionic bond,[17] B3LYP is a better method to calculate the RESP charges. For our test job of cytosine, the RESP charges derived from HF/6-31G* and B3LYP/6-31+G* produced a root sum-of-squares deviation (RSSD) of only 0.071 e for all the charges.

In the MD simulation, only the RESP charges of the substrate, intermediates, and products, as well as those of the Zn-bound water, Zn, and the *side chains* of His62, Cys91, and Cys94, are reevaluated by our quantum chemical calculations relative to

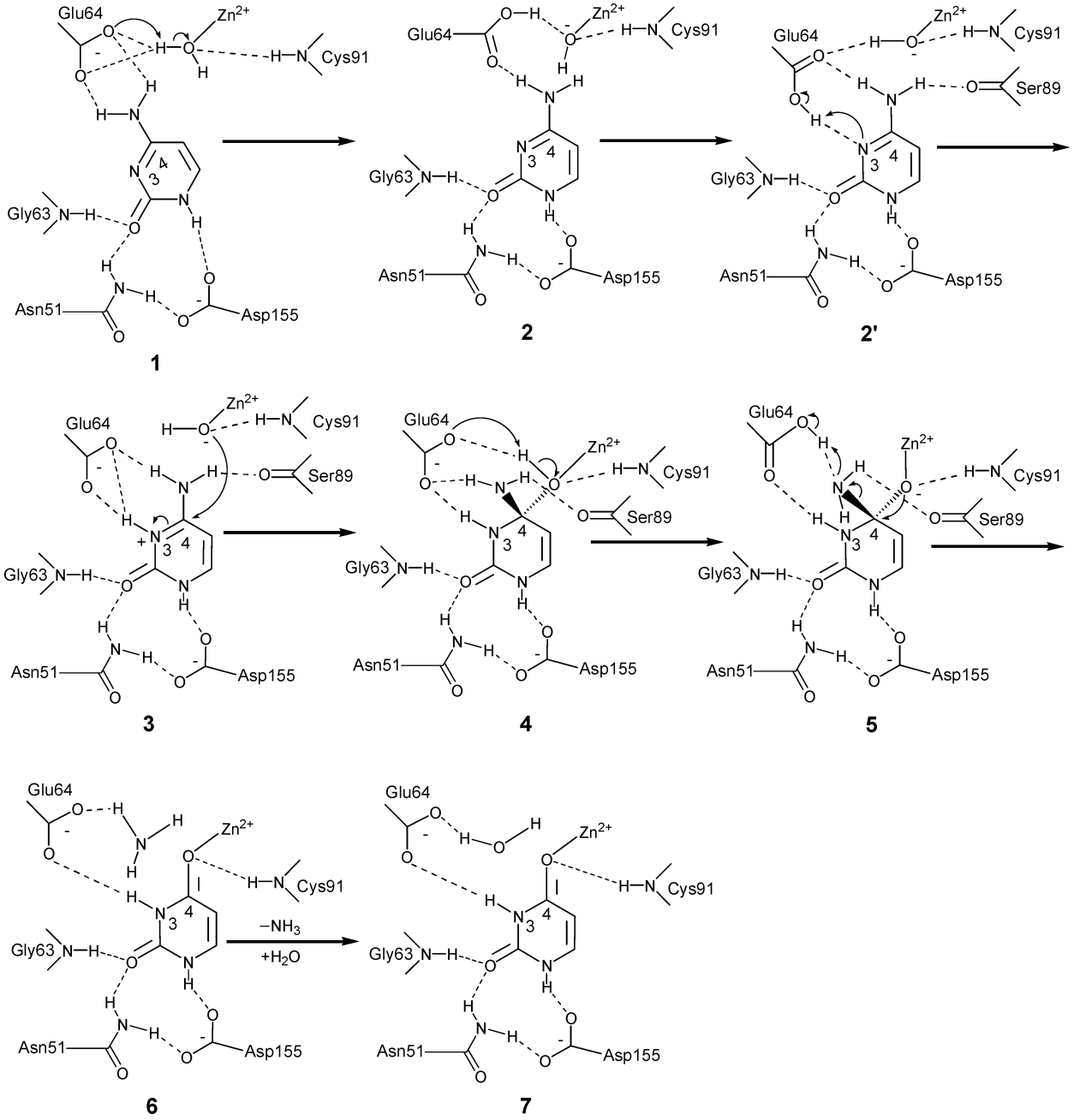

Figure 2. Schematic representation of the path of the yCD-catalyzed reaction as revealed by our quantum chemical calculations[8] and molecular dynamic simulations (this work): (**1**) water/cytosine active site, (**2**) hydroxide/Glu64H cytosine complex, (**3**) hydroxide/Glu64 cytosine−H complex, (**4**) intermediate I complex, (**5**) intermediate II complex, (**6**) uracil/ammonia complex, (**7**) uracil/water complex.

TABLE 1: Force Constants for the Zn Complex

K_r (kcal/mol−Å^2)			
Zn−S	Zn−O	Zn−N	
300	300	300	
K_θ (kcal/mol-rad^2)			
S−Zn−S	S−Zn−O	S−Zn−N	O−Zn−N
75	75	75	75
Zn−O−C	Zn−S−C	Zn−O−H	Zn−N−C
35	35	35	35

their values in the AMBER database. The charges listed in Table 2 are slightly modified to preserve the charge neutrality of the Zn complex. Charges of Asp155, and the backbone charges of His62, Cys91, and Cys94 are the same as those from the AMBER database. Because no new bond, bond angle, or dihedral angle parameterization was performed for this system in our calculations, this procedure was used to minimally perturb the parameters from the AMBER database.

MD Simulation of the Free Form of yCD. Starting coordinates for the protein atoms were taken from the free form of yCD at 1.43-Å resolution crystal structure.[4] There is a second Zn in the active site of the crystal structure, which was deleted for the simulations. All the crystal water molecules were removed except the one bound to the catalytic Zn. The protonation states of the ionizable residues were set to their normal values at pH 7. The protein was surrounded by a periodic box of 12.5 Å (∼17 000) TIP3P water molecules. Na^+ ions were placed by the Leap program[15] to neutralize the −6 charge of the model system. The parm94 version of the all-atom AMBER force field[18] was used for all the simulations.

TABLE 2: Charges (e units) of Zn Complex Used in the yCD Simulations

	1[a]	2[b]	3[c]	4[d]	5[e]	6[f]
			His62			
CB	−0.168	−0.420	−0.708	0.047	0.129	−0.278
HB2	0.082	0.105	0.266	0.063	0.045	0.150
HB3	0.082	0.105	0.266	0.063	0.045	0.150
CG	0.258	0.241	0.284	0.005	−0.051	0.074
ND1	−0.283	−0.111	−0.303	−0.168	−0.159	−0.143
CE1	−0.061	−0.195	0.021	−0.100	−0.082	−0.019
HE1	0.120	0.175	0.159	0.168	0.169	0.133
NE2	0.071	0.002	−0.336	−0.086	−0.119	−0.097
HE2	0.233	0.276	0.416	0.326	0.335	0.281
CD2	−0.427	−0.401	−0.168	−0.323	−0.291	−0.342
HD2	0.313	0.268	0.195	0.218	0.220	0.254
			Cys91/Cys94			
CB	0.221	−0.006	0.215	0.08	0.059	0.027
HB2	−0.035	0.016	−0.056	0.019	0.026	−0.002
HB3	−0.035	0.016	−0.056	0.019	0.026	−0.002
SG	−0.644	−0.568	−0.729	−0.703	−0.723	−0.673
			Zn			
Zn	0.762	0.609	1.027	0.876	0.887	0.668

[a] Data used in free form and water/cytosine active site simulations. [b] Data used in intermediate analogue complex simulation. [c] Data used in hydroxide/Glu64H cytosine complex and hydroxide/Glu64 cytosine−H complex simulations. [d] Data used in intermediate I complex simulation. [e] Data used in intermediate II complex simulation. [f] Data used in product uracil/ammonia (and uracil/water) complex.

MD simulations were carried out using the SANDER module in *AMBER 7.0*.[16] The SHAKE algorithm[19] was used to constrain all bond lengths involving hydrogen atoms permitting a 2-fs time step. A nonbonded pair list cutoff of 8.0 Å was used, and the nonbonded pair list was updated every 25 steps. The Particle-Mesh-Ewald method was used[20] to evaluate the contributions of the long-range electrostatic interactions. The pressure (1 atm) and the temperature (300 K) of the system were controlled during the MD simulations by Berendsen's method.[21] The typical simulation time was 2 ns, with a 500-ps equilibration period. Coordinates are saved every 2 ps. All of the MD results were analyzed with the PTRAJ module of *AMBER 7.0*. In these analyses, we assign hydrogen bonds when the distance of two heavy atoms (O or N) is less than 3.2 Å and the angle (heavy-atom−hydrogen−heavy-atom) is greater than 120°.

MD Simulation of the yCD Intermediate Analogue Complex. The starting structure for the yCD intermediate analogue complex simulation was taken from the crystal structure.[4] Subunit 1 has 156 residues (the first 2 are missing); subunit 2 has 161 residues, because 3 extra residues are attached to the N-terminus. One more residue, Glu64, is included in the charge parameterization, because it forms a strong hydrogen bond with the ligand in the crystal structure, and the inclusion of this residue may influence the RESP charges of the Zn-bound complex. The Glu64 charges used in the MD are the AMBER ones, because they are very close to those from the quantum chemical calculation. The MD simulation protocols for the yCD intermediate analogue were identical to those for the unbound model, except the modeled system was maintained at constant volume and temperature, as was the case for the other simulations described below.

MD Simulation of the yCD Water/Cytosine Complex (1 in Figure 2). Cytosine was docked to the yCD free enzyme crystal structure active site in the same position found for the intermediate analogue. The Zn-bound water molecule was included in the simulation. All other crystal water molecules and the second Zn were removed, as in the free-form simulation. The force-field parameters of the yCD protein are the same as in the free yCD simulation. The RESP charges of cytosine are from an HF/6-31G* calculation.

MD Simulation of the yCD Hydroxide/Glu64H Cytosine Complex (2 in Figure 2). The 500-ps instantaneous structure of the yCD water/cytosine system was adopted as the starting structure of the yCD hydroxide/cytosine system. The deprotonated Glu64 was mutated into a protonated glutamic acid, while the Zn-complex water was mutated into a hydroxide group in this system. The new RESP charges of the Zn complex (Zn, His62, Cys91, Cys94, and the hydroxide ligated to Zn) were calculated on the basis of a free-form ONIOM(B3LYP:PM3) minimized structure with the proton restrained to Glu64.[8]

MD Simulation of the yCD Hydroxide/Glu64 Cytosine−H Complex (3 in Figure 2). The 1.0-ns snapshot structure of the yCD hydroxide/Glu64H cytosine system was used as the starting structure of yCD hydroxide/Glu64 cytosine−H system. The proton of Glu64 was transferred to the N3 of cytosine in this system. The RESP charges of the Zn complex (Zn, His62, Cys91, Cys94, hydroxide) are the same as the yCD hydroxide/Glu64H cytosine complex simulation, and the RESP charges of protonated cytosine were calculated on the basis of the HF/6-31G* QM calculation.

MD Simulation of the yCD Intermediate Complexes (4 and 5 in Figure 2). The starting structure for the yCD intermediate complex simulation was taken from the crystal structure of the yCD intermediate analogue complex. The intermediate was docked to the same position where the intermediate analogue stays. Because the intermediate could be either protonated, intermediate I, (with deprotonated Glu64, **4** in Figure 2) or deprotonated, intermediate II, (with protonated Glu64, **5** in Figure 2), two situations were implemented in the two different active sites. The RESP charges (see Table 2) of these two Zn complexes were calculated on the basis of the yCD intermediate analogue crystal structure.

MD Simulation of the yCD Product Complexes (6 and 7 in Figure 2). The starting structure for the yCD product complex simulation was taken from the yCD intermediate analogue complex crystal structure. Intermediate II was converted to uracil/ammonia. Because our ONIOM(B3LYP:PM3)[8] calculations showed that the Zn complex structure in this system was similar to that in the crystal structure of yCD intermediate analogue complex, uracil was bound to the Zn atom for the simulation with a bond to the oxygen. This geometrical arrangement is similar to the cytidine deaminase−uridine complex crystal structure.[7] The new RESP charges of the Zn complex were calculated. To study the release of ammonia and its possible exchange with water in the active site, ammonia was substituted by water in one active site, while it was kept in the other.

Potential of Mean Force (PMF) Calculation of Glu64 COOH Rotation in the yCD Hydroxide/Glu64H Cytosine Complex. The simulations that we carry out show that the Glu64 (GluH64) carboxylate (carboxylic acid) moiety fluctuates around three orientations, which can be described by the dihedral angle φ defined by the CB−CD−CG−OE2 atoms of Glu64. The free energy of rotation was obtained from the potential of mean force (PMF) $W(\varphi)$ that is related to the probability $P(\varphi)\,d\varphi$ of finding the dihedral angle between φ and $(\varphi + d\varphi)$ according to $W(\varphi) = -k_BT \ln P(\varphi)$. The PMF was obtained by a free energy umbrella sampling method[22,23] in which a series of harmonic restraint terms (windows) are added to the system's Hamiltonian in order to force the system to sample the desired regions of φ space, in this manner overcoming the poor sampling of high-energy conformations that would occur in an unbiased MD

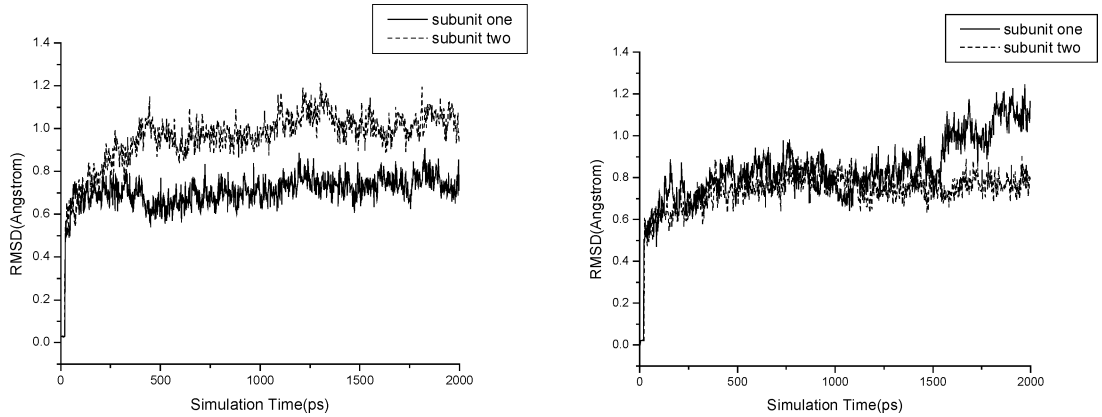

Figure 3. RMSDs of CA (residues 15−158) for subunit 1 and subunit 2 compared with the corresponding crystal structures. The first 500 ps were treated as an equilibration stage, while the last 1500 ps were used to do the data analysis. Left panel: free form. Right panel: intermediate analogue complex.

trajectory. The data from the windows were combined using the weighted histogram analysis method (WHAM)[24] to produce the PMF over the desired range of φ. The force constant was set to 20 kcal/(mol-rad^2), which provides a rms restraint potential window width of approximately 10°, and the window size was set to 3.5° to ensure good overlap of data in neighboring windows. The PMF between states 1 and 2 was determined by running the simulations forward and backward with 5 ps of equilibration and 5 ps of data collection for each window (total of 40 windows). The parameters we used were validated by testing the accuracy of the method on the dihedral PMF for ethane solvated in water. The results (not shown) indicate that this set of parameters can reproduce the PMF of the ethane dihedral rotation quite well. By using this set of parameters, our forward and backward simulations of the Glu64 CB−CG−CD−OE2 dihedral rotation gave consistent results (see Results and Discussion). The PMF between states 2 and 3 was determined by starting the simulation from state 2.

Chemical Alchemy Simulation of NH_3 and H_2O Exchange. Our ONIOM(B3LYP:PM3)[8] calculations indicate that uracil is released by an oxygen exchange mechanism that uses a water molecule at the same location as the product ammonia in the active site. As a consequence, before the release of uracil, ammonia should exchange with the water molecule. Therefore, we evaluated the difference in binding free energy between water and ammonia by mutating water to ammonia (and ammonia to water) in both the protein active site and the water solution. The RESP charges of ammonia were calculated on the basis of an HF/6-31G* calculation. After ammonia was solvated in water (box side of 12.5 Å) and equilibrated, it was mutated to a water molecule. The nitrogen and two ammonia hydrogen atoms were mutated to an oxygen atom and two water hydrogens, while the third hydrogen was mutated to a dummy atom that has zero charge and zero van der Waals radius but maintains its internal interaction parameters. Twelve windows were used with 30 ps per window (15 ps for equilibration and 15 ps for data collection). SHAKE was not used, considering that mutation of hydrogen atoms is involved, necessitating a time step reduction to 1 fs. Gaussian quadrature formulas were used to pick values for the ranges of these windows. The same procedure was used to mutate water (with a dummy atom attached) to ammonia. Thermodynamic integration was used to do the free energy calculation. The contribution to the free energy from the dummy atom was evaluated analytically.[25] A standard state of 1 M (1661 Å^{-3}) was used for the free dummy atom. The results for the forward and backward mutation show excellent consistency (see Results and Discussion).

TABLE 3: RMSD for Free and Intermediate Analogue Complex Forms

	RMSD (Å)			
	free form		intermediate analogue complex	
	subunit 1	subunit 2	subunit 1	subunit 2
CA	0.72 (0.06)	1.01 (0.07)	0.90 (0.14)	0.77 (0.05)
total[a]	1.29 (0.06)	1.60 (0.07)	1.46 (0.11)	1.24 (0.05)
N-terminal	2.28 (0.24)	3.43 (0.78)	2.65 (0.32)	3.66 (0.96)
C-terminal	0.98 (0.11)	1.50 (0.11)	1.40 (0.37)	1.32 (0.23)
loop	1.41 (0.19)	1.93 (0.22)	1.97 (0.32)	1.20 (0.09)

[a] Not including residues 1−14.

In the yCD product simulation, the water and the ammonia were put into different active sites, and they were mutated to each other, respectively, by the procedure outlined above. The free energy difference in water and protein is the binding free energy. Assuming a small effect from the different active sites, the difference in binding free energies between water and ammonia is then available.

III. Results and Discussion

yCD Free and Intermediate Analogue Complex Compared with the Crystal Structures. yCD is a homodimer with 158 residues per subunit. Each subunit has 1 active site that is covered by Phe114 located in a loop consisting of residues 109−116 and by Trp152 and Ile156 contained in the C-terminal helix, residues 149−158. The data analysis is based on individual subunits in order to get better statistics, because the crystal structure shows that the configurations of the two subunits are the same, except for the N-terminus (∼10 residues). We superimpose the MD snapshots on the crystal structure without using the N-terminal 14 residues.

The time evolution of the CA atom RMSD of the instantaneous structures (not including the first 14 residues) from the initial crystal structure for the free yCD and the intermediate analogue complex indicate that the two systems are in equilibrium with respect to the rms deviations during the analyzed trajectory (Figure 3). The mass-weighted RMSD of all atoms relative to the crystal structure is, on average, 1.29 Å for subunit 1 and 1.60 Å for subunit 2, in the free-form simulation (Table 3), indicating that the structural changes in the protein were not large during the course of the simulation. The different RMSDs do indicate that some part of the protein in subunit 2 moved further away from the crystal structure than did the protein in subunit 1. By superimposing the average structure

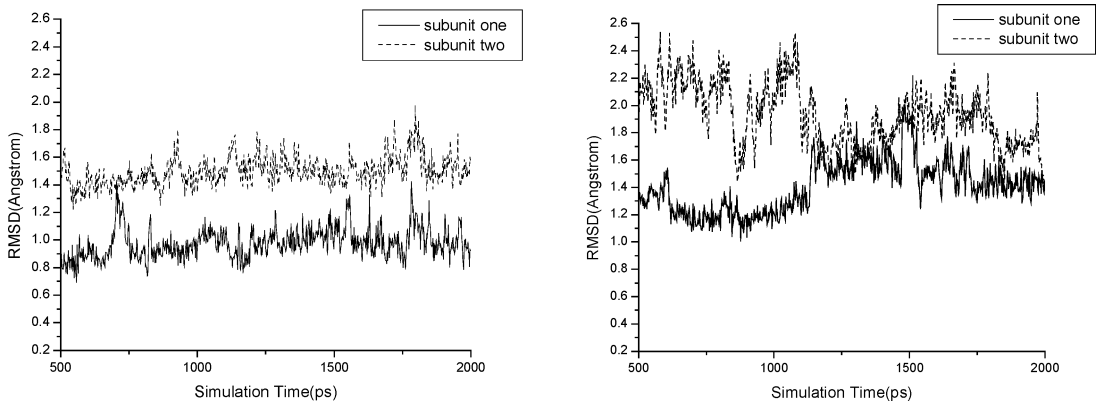

Figure 4. RMSDs from the crystal structure of (a) the C-terminal helix (left panel) and (b) the Phe114 loop (right panel) in the free yCD simulation, after equilibration.

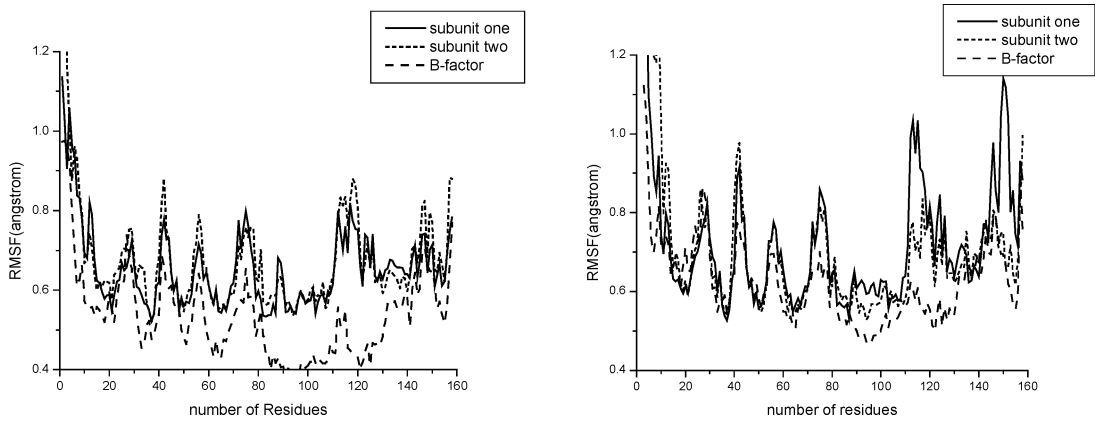

Figure 5. RMSFs of CAs in the yCD simulations compared with the crystal structure B-factors. (a) Left panel: free yCD simulation. (b) Right panel: yCD intermediate analogue complex.

of subunit 1 and subunit 2 (data not shown), we see that the largest differences are in the N-terminal, C-terminal, and Phe114 loop regions. The average RMSD data also suggest distinctions among these three regions (Table 3). The time evolution of the RMSD of the C-terminal helix shows that two substates were captured in the free yCD MD simulation (Figure 4a). Subunit 1 maintains the crystal structure of the C-terminal helix, while subunit 2 shifted the whole helix slightly away, and this movement lets the Trp152 side chain occupy the active site. This movement is not surprising, because in the crystal structure, one additional Zn atom, which is bridged by a water molecule to the active site Zn, coordinates with three more water molecules.[4] This Zn complex fills the active site; in the MD simulation, the extra Zn with its coordinated waters was removed, providing space for some rearrangement around the active site.

Interestingly, the apo and intermediate complex forms have essentially the same crystal structure,[4] with a closed active site. Ligands cannot move in or out without moving the covering residues Phe114, Trp152, and Ile156. The time evolution of the Phe114 loop RMSD in the free-form simulation highlights the difference in this region between subunit 1 and subunit 2 (Figure 4b). The Phe114 loop region is flexible, though a 2-ns simulation may not be long enough to describe a motion that could permit substrate entrance. To gain insight into the fluctuations of the yCD enzyme, the rms fluctuation (RMSF) was calculated by comparing the instantaneous protein structure with the average one for the free form (Figure 5a). Though the difference in RMSD is large between subunit 1 and subunit 2 compared with the crystal structure, the RMSFs for CA atoms are almost the same, and consistent with the crystal B-factors. The residue RMSF values are quite small (most of them are around 0.5 Å), which indicates that the yCD protein is quite rigid as a whole in the free form on the MD time scale.

As in the free-form enzyme, the N-terminal residues are far more flexible than the rest of the protein in the intermediate analogue complex (Table 3). The total RMSDs (not including N-terminal 14 residues) are 1.46 Å for subunit 1 and 1.24 Å for subunit 2, quite similar to the free-form values. The small RMSF values for the CA atoms indicate the rigidity of the intermediate analogue complex on the MD time scale as well (Figure 5b). The differing RMSFs between subunits 1 and 2 (Figure 5b) in the intermediate analogue complex are evidence that two different configurations are being accessed, at least on the 2-ns time scale. The results indicate that the Phe114 loop and the C-terminal helix are flexible, especially in subunit 1, relative to the crystal structure.

Structure of the Active Site. A schematic representation and a typical snapshot of the active site of the apo and intermediate analogue complex are displayed in Figure 6. In Table 4, the most significant H-bonds between the ligand (or Zn-bound water in the free form) and the enzyme residues are characterized in terms of the distances between two heavy atoms and their percentages of occurrence. In the free-form simulation, the Zn-bound water forms hydrogen bonds with OE1 and OE2 of Glu64, which are not present in the crystal structure, because the second Zn in the crystal structure blocks the formation of these hydrogen bonds. In the MD simulation, this second Zn is not present. There is ∼70% hydrogen bond occurrence for OE2 of Glu64 and ∼30% for OE1 in subunit 2, which indicates that the carboxyl group of Glu64 can rotate in the free-form simulation (Figure 7a). In the complex, the ligand forms

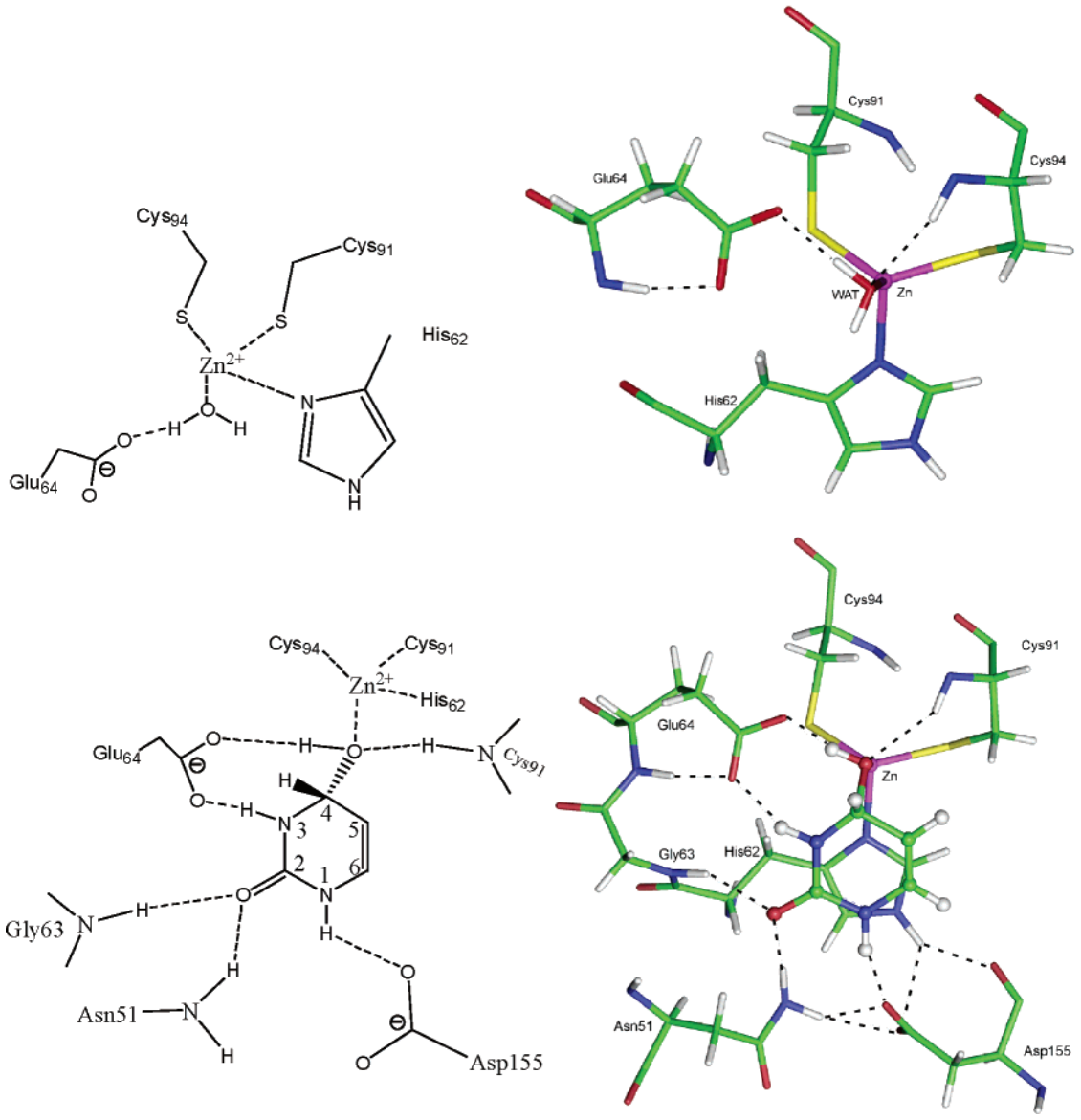

Figure 6. Schematic representation and MD snapshots of the yCD active site. Top panel: free form. Bottom panel: intermediate analogue complex form.

hydrogen bonds with Asn51, Gly63, Glu64, Cys91, and Asp155. The simulation results are in excellent agreement with the hydrogen-bond network found in the crystal structure (Table 4), which supports the Zn-complex parameters and MD protocols developed for this simulation.

Orientational Changes of Cytosine along the Reaction Path. Snapshots of the active site of the yCD water/cytosine reactant complex show, surprisingly, that cytosine rotates around the axis perpendicular to its pyrimidine ring to move its NH_2 group closer to the Glu64 carboxyl group (**1** in Figure 2), relative to its starting position that is the same as the intermediate analogue complex orientation in the crystal structure. This rotation helps the NH_2 group of cytosine form a hydrogen-bond network with Glu64 (Table 5). The upper part of the pyrimidine ring moves away from the Zn-bound water, because of the van der Waals repulsion between them, while the bottom part is restrained by three hydrogen bonds between cytosine and Gly63, Asn51, and Asp155. The distance between C4 of cytosine and O of the Zn-bound water is 3.26 ± 0.17 Å in subunit 1 and 3.19 ± 0.14 Å in subunit 2. Cytosine orients somewhat differently in the two subunits (Table 5). The NH_2 group of cytosine in subunit 1 points directly at the carboxyl group of Glu64 and forms a hydrogen-bond network using the two carboxylate oxygens and two amino hydrogens. But in subunit 2, NH_2 can also form a hydrogen bond with O of Ser89 that is oriented toward the upper right side of cytosine.

After protonation of Glu64 by proton transfer from the Zn-bound water (yCD hydroxide/Glu64H cytosine model, **2** in Figure 2), cytosine rotates back to the orientation of the intermediate analogue found in the crystal structure[4] in the MD simulation. In this system, the protonated Glu64 forms one hydrogen bond with the amino group of cytosine instead of the hydrogen-bond network as in the previous carboxylate system (Table 6). The starting structure for this simulation was taken from one snapshot of the yCD water/cytosine simulation, with slightly different geometries in subunits 1 and 2. Correspondingly, these produce slightly different active-site interactions. Notably, the distance between C4 of cytosine and O of the Zn-bound hydroxide is 3.02 ± 0.13 Å in subunit 1, but 3.33 ± 0.20 Å in subunit 2. By superimposing the average structures of subunits 1 and 2, we found that the cytosine in subunit 2 was pushed down by ~0.5 Å relative to that of subunit 1. This

TABLE 4: Hydrogen Bonds in yCD Free and Intermediate Analogue Complex Forms

	occurrence (%)	distance (Å)	crystal structure (Å)
Subunit 1			
intermediate analogue complex form			
Asn51-NH...O2	99.47	2.82 (0.10)	3.14
Asp155-OD...H−N1	100.00	2.70 (0.08)	2.69
Gly63-NH...O2	92.68	2.94 (0.12)	2.89
Glu64-OE1...H−O4	37.42	3.06 (0.11)	3.34
Glu64-OE2...H−O4	99.73	2.50 (0.07)	2.49
Cys91-NH...O4	22.90	3.10 (0.07)	3.02
Glu64-OE1...H−N3	99.87	2.79 (0.09)	2.80
free form			
Glu64-OE2...H−WAT	100.00	2.62 (0.10)	
Subunit 2			
intermediate analogue complex form			
Asn51-NH...O2	98.80	2.85 (0.11)	2.90
Asp155-OD...H−N1	100.00	2.69 (0.07)	2.69
Gly63-NH...O2	89.21	2.97 (0.12)	2.87
Glu64-OE1...H−O4	39.41	2.95 (0.24)	3.37
Glu64-OE2...H−O4	95.61	2.53 (0.11)	2.52
Cys91-NH...O4	21.04	3.12 (0.06)	3.03
Glu64-OE1...H−N3	91.48	2.80 (0.09)	2.78
free form			
Glu64-OE2...H−WAT	73.60	2.57 (0.10)	
Glu64-OE1...H−WAT	28.93	2.60 (0.16)	

is consistent with the formation of a hydrogen bond between the carbonyl O of Ser89 and the amino group of cytosine in subunit 1, but not in subunit 2 (Table 6). The orientation of protonated Glu64 is also more favorable for proton transfer to the N3 of cytosine in subunit 1 than in subunit 2 (see discussion below).

After Glu64 transfers a proton to the N3 of cytosine (yCD hydroxide/Glu64 cytosine−H), the distance between the C4 of cytosine and the O of Zn-bound hydroxide becomes 2.84 Å in subunit 1 and 2.80 Å in subunit 2; these distances are about 0.4 Å shorter than in the initial yCD cytosine complex. Thus, the C4 atom of cytosine becomes well-positioned for nucleophilic attack by the hydroxide. Therefore, after proton transfer from the Zn-bound water to the N3 atom, the reorientation of cytosine makes nucleophilic attack of the Zn-bound hydroxide group on C4 easier.

The Proton Shuttle with Glu64. Our quantum chemical calculations indicate that Glu64 in yCD acts as a proton shuttle with the Zn-ligated water.[8] In the free-form crystal structure, there is a second Zn that pushes Glu64 away from this water molecule, which makes proton transfer from it to Glu64 improbable. In the free-form MD simulation, where this second Zn atom was removed, the OE1 or OE2 of Glu64 forms a strong hydrogen bond with the Zn-bound water, with distance of ∼2.60 Å in both subunit 1 and subunit 2 (Table 4). Interestingly, the side-chain carboxyl group of Glu64 can rotate in subunit 2 despite the strong hydrogen bond (Figure 7a). Our calculations[8] indicate that, in the apo enzyme, the proton stays covalently bound to the water, versus transferring to protonate Glu64.

After cytosine binds to the protein (yCD water/cytosine model, **1** in Figure 2), Glu64 still forms a strong hydrogen bond with the Zn-bound water (with distance OE1...O of 2.59 Å or OE2...O of 2.60 Å) in subunit 1 and OE2...O of 2.60 Å in subunit 2 (Table 5). The difference between them comes from the rotation of the Glu64 carboxyl group in subunit 1 but not in subunit 2 (Figure 7b). As discussed above, after the proton transfers from Zn-bound water to the carboxyl O of Glu64, the simulation (yCD hydroxide/Glu64H cytosine model, **2** in Figure 2) shows a slightly different active site conformation in subunit

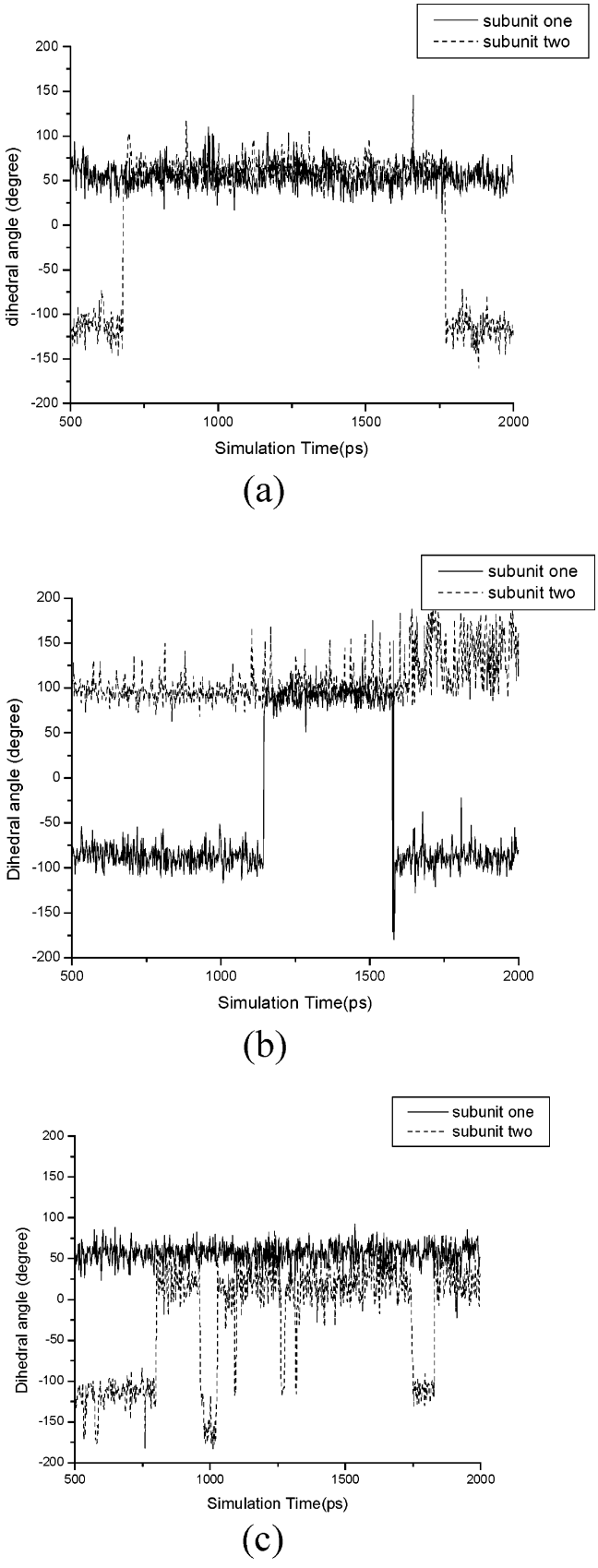

Figure 7. Changes in the CB−CG−CD−OE1 dihedral angle of Glu64. (a) Free yCD MD simulation. (b) yCD water/cytosine model (see **1** in Figure 2). (c) yCD intermediate I complex (see **4** in Figure 2).

1 and subunit 2. The apparent difference is attributable to the dihedral angle φ formed by the Glu64H CB−CG−CD−OE2 atoms with $\varphi \approx 0°$ (all four atoms in the same plane with the

TABLE 5: Hydrogen Bonds in yCD Water/Cytosine Simulation

	occurrence (%)	distance (Å)	occurrence (%)	distance (Å)
	subunit 1		subunit 2	
Asn51-NH...O2	99.73	2.82 (0.10)	99.60	2.84 (0.11)
Asp155-OD...H−N1	99.07	2.84 (0.11)	100.00	2.79 (0.10)
Gly63-NH...O2	75.87	2.99 (0.12)	84.80	2.97 (0.12)
Glu64-OE1...H1−N4	8.27	2.94 (0.12)	88.00	2.88 (0.13)
Glu64-OE1...H2−N4	32.93	2.87 (0.14)		
Glu64-OE2...H1−N4	23.20	2.86 (0.13)	9.33	3.04 (0.10)
Glu64-OE2...H2−N4	50.67	2.84 (0.13)	31.07	2.88 (0.13)
Glu64-OE1...H−WAT	70.80	2.59 (0.09)		
Glu64-OE2...H−WAT	29.33	2.60 (0.09)	100.00	2.60 (0.10)
Cys91-NH...O−WAT	98.93	2.92 (0.10)	98.40	2.91 (0.09)
Ser89-O...H2−N4			49.20	2.91 (0.13)

TABLE 6: Hydrogen Bonds in yCD Hydroxide/Glu64H Cytosine Simulation

	occurrence (%)	distance (Å)	occurrence (%)	distance (Å)
	subunit 1		subunit 2	
Asn51-NH...O2	92.67	2.91 (0.12)	98.67	2.84 (0.11)
Asp155-OD...H−N1	99.33	2.78 (0.10)	36.27	2.79 (0.11)
Gly63-NH...O2	89.33	2.96 (0.12)	63.47	3.01 (0.11)
Glu64-OE1...H1−N4	79.73	2.94 (0.13)	79.33	2.90 (0.13)
Glu64-OE2H...OH	97.73	2.60 (0.10)	99.87	2.62 (0.10)
Cys91NH...OH	99.07	2.91 (0.10)	90.40	2.99 (0.11)
Ser89-O...H2−N4	79.33	2.96 (0.12)		

terminal atoms cis for subunit 1, which we shall refer to as state 1) and $\varphi \approx 120°$ for subunit 2 (state 2). In state 1, the C−OE1−OE2−H plane is close to parallel with the cytosine pyrimidine ring plane and OE2−H is hydrogen-bonded to the Zn-bound hydroxide group as a donor. In state 2, the angle between these two planes is about 60° with the OE2−H hydrogen-bonded to the same hydroxide group. In both cases, this hydrogen bond is quite strong, with distance OE2...O of 2.60 Å in subunit 1 and 2.62 Å in subunit 2. However, the ONIOM calculation[8] indicates that these two protonated Glu64s are not stable states unless the OE2−H points to N3 of cytosine and forms a hydrogen bond with it (**2′** in Figure 2), instead of pointing to the O atom of the Zn-bound hydroxide. This could be done simply by rotating the dihedral angle CB−CG−CD−OE2 of Glu64 to $\varphi \approx -50°$. This geometry defines state 3, where OE2−H points to N3 and the C−OE1−OE2−H plane is again parallel with the cytosine pyrimidine ring.

From the MD perspective, where chemical species are fixed during a simulation, state 1 and state 2 can be stable in the sense of corresponding to minima on a free energy surface. Therefore, it is of interest to determine the PMF $W(\varphi)$ along the Glu64H carboxyl dihedral coordinate, φ, formed by the atoms CB−CG−CD−OE2. The umbrella sampling method that we use to obtain the PMF is described in the Methods section. Figure 8 displays the PMF and shows that state 3 is only 2 kcal/mol higher than state 1. Because state 3 is a not a minimum of $W(\varphi)$, configurations where the Glu64 carboxyl OH point toward the cytosine N3 atom in the simulation trajectory are transient. State 2 has the lowest free energy, but the barrier to rotate from state 2 to state 1 is about 6 kcal/mol, and that makes the dihedral angle rotation somewhat difficult. The rotation frequency estimated from transition-state theory is around 0.5 ns^{-1}, and this frequency is consistent with the one- or no-transition behavior observed in Figure 7. Thus, it is more likely that a proton transfers from the Zn-bound water to form Glu64 carboxyl OH, followed by a dihedral angle CB−CG−CD−OE2 rotation of ∼50° to form a stable state with the Glu64 OE2H pointing to the N3 of cytosine. That the MD force field does not produce a stable state for state 3 may be a consequence of

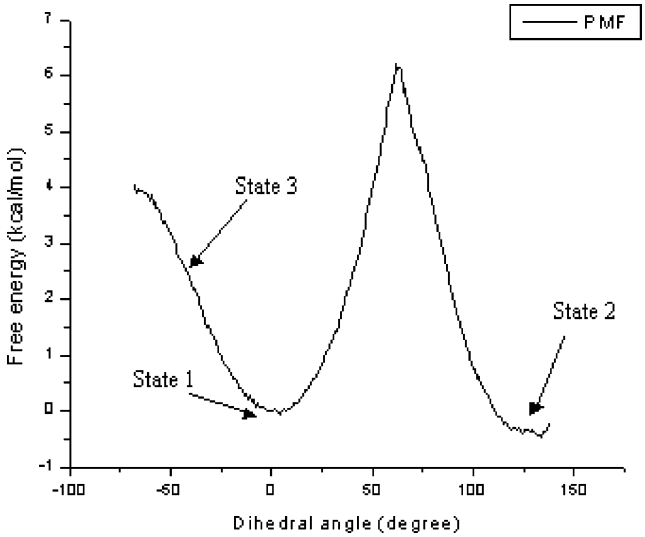

Figure 8. Potential of mean force for rotation around the CB−CG−CD−OE2 dihedral angle of Glu64H.

TABLE 7: Hydrogen Bonds in yCD Hydroxide/Glu64 Cytosine−H Simulation

	occurrence (%)	distance (Å)	occurrence (%)	distance (Å)
	subunit 1		subunit 2	
Asn51-NH...O2	63.73	3.03 (0.11)	74.53	2.99 (0.11)
Asp155-OD...H−N1	100.00	2.70 (0.08)	100.00	2.71 (0.08)
Gly63-NH...O2	54.27	3.04 (0.10)	82.00	2.99 (0.11)
Glu64-OE1...H1−N4	100.00	2.73 (0.08)	99.87	2.72 (0.07)
Glu64-OE1...H−N3	44.67	3.07 (0.10)	38.40	3.07 (0.10)
Glu64-OE2...H−N3	99.87	2.80 (0.09)	100.00	2.79 (0.09)
Cys91NH...OH	100.00	2.82 (0.08)	100.00	2.83 (0.08)
Ser89-O...H2−N4	80.00	2.87 (0.13)	91.60	2.84 (0.12)

the deficiency of the force field, or it may reflect the short time scale of the simulation that is used to construct the PMF. After the proton transfers from Glu64 to the N3 of cytosine (Figure 1b), a 2-ns simulation of the yCD hydroxide/Glu64 cytosine−H complex (**3** in Figure 2), as described in the Methods section, was carried out. A hydrogen-bond analysis of the trajectory shows that the Glu64 carboxyl group forms a stable hydrogen bond with the amino group of cytosine in both subunit 1 and subunit 2 (Table 7). Importantly, the geometry enforced by this new hydrogen bond places C4 of cytosine in a favorable position for nucleophilic attack by the Zn-bound hydroxide (The O−C4 distance is ∼2.8 Å in both active sites.).

Following the nucleophilic attack of the Zn-bound hydroxide group on C4 of cytosine, the proton of the hydroxide group (now C4OH) could either stay with the tetrahedral intermediate I (**4** in Figure 2) or transfer to the Glu64 intermediate II (**5** in Figure 2). The intermediate I (intermediate II) state was modeled in the active site of subunit 1 (2) (see Methods section), and a new MD simulation (yCD intermediate model) was performed. In the intermediate I state (Table 8), both OE1 and OE2 of Glu64 can form hydrogen bonds with N3 and NH_2 of intermediate I, which indicates that the carboxyl group of Glu64 can once again rotate during the simulation (Figure 7c). The Glu64 carboxylate forms a strong hydrogen bond with C4OH (distance of 2.65 Å), suggesting that it is easier for the C4OH proton to transfer to the carboxyl group of Glu64 than to some other residue. After this proton transfer, to form the intermediate II state, the Glu64 OE2H forms hydrogen bonds with both N4 and O4, with a slight preference for N4 (occurrence of 100%, distance of 2.72 Å) than O4 (occurrence of 84%, distance of 2.83 Å), as shown in Table 8. Therefore, in a manner similar to

TABLE 8: Hydrogen Bonds in yCD Intermediate I/II Simulations

	occurrence (%)	distance (Å)	occurrence (%)	distance (Å)
	intermediate I		intermediate II	
Asn51-NH...O2	99.07	2.86 (0.11)	100.00	2.84 (0.10)
Asp155-OD...H−N1	100.00	2.70 (0.08)	100.00	2.76 (0.09)
Gly63-NH...O2	88.00	2.97 (0.12)	89.07	2.96 (0.12)
Glu64-OE1...H1−N4	22.93	3.02 (0.10)		
Glu64-OE2...H1−N4	49.07	3.02 (0.11)		
Glu64-OE1...H−O4	34.80	2.65 (0.19)		
Glu64-OE2-H...O4			83.60	2.83 (0.13)
Glu64-OE2-H...N4			100.00	2.72 (0.11)
Glu64-OE1...H−N3	30.80	2.86 (0.10)	100.00	2.83 (0.10)
Glu64-OE2...H−N3	69.47	2.84 (0.10)		
Cys91NH...O4	96.13	2.97 (0.10)	97.47	2.96 (0.11)
Ser89-O...H2−N4	40.27	3.03 (0.11)	36.67	3.06 (0.10)

TABLE 9: Hydrogen Bonds in yCD Uracil/Ammonia and Uracil/Water Simulations

	occurrence (%)	distance (Å)	occurrence (%)	distance (Å)
	uracil/ammonia		uracil/water	
Asn51-NH...O2	97.87	2.87 (0.12)	96.93	2.88 (0.12)
Asp155-OD...H−N1	100	2.69 (0.08)	100.00	2.70 (0.07)
Gly63-NH...O2	79.2	2.99 (0.11)	87.60	2.98 (0.12)
Glu64-OE2...H−N3	99.87	2.83 (0.09)	99.07	2.86 (0.11)
Cys91NH...O4	60.27	3.07 (0.09)	45.2	3.08 (0.08)
Glu64-OE1...H1−NH3/(H1−WAT)	94.67	2.84 (0.11)	100.00	2.65 (0.11)
Ser89-O...H2−NH3/(H2−WAT)	14.53	3.05 (0.10)	23.47	2.81 (0.17)

the first proton transfer, after Glu64 receives the proton, Glu64 CB−CG−CD−OE2 rotates to point OE2H to N4.

In summary, along the reaction path, the rotation of the Glu64 dihedral CB−CG−CD−OE2 is critical for enabling the various proton transfers required to form intermediate II. The free energy simulations show that such rotations can happen on a nanosecond time scale and suggest that Glu64 acts as a proton shuttle multiple times.

The Hydrogen-Bond Network. In addition to the critical interactions between Glu64, the Zn-coordinated water, or hydroxide, and the substrate, intermediates, or products, the enzyme maintains a network of hydrogen bonds for substrate binding and catalysis. The hydrogen bonds involving the side-chain amide of Asn51, the NH's of Gly63 and Cys91, and the carboxylate of Asp155 are maintained throughout the reaction path (Figure 2 and Tables 5−9). These hydrogen bonds help to stabilize all the complexes in the reaction path and therefore are important for both substrate binding and catalysis. In particular, the hydrogen bond between the NH group of Cys91 and the Zn-bound water (or hydroxide) may acidify the latter group and facilitate the proton transfers to Glu64. The hydrogen bond between the carbonyl O of Ser89 and the amino group of cytosine evolves during the reaction. The hydrogen bond is strongest in terms of both geometry and frequency of occurrence in the yCD hydroxide/Glu64 cytosine−H complex (**3** in Figure 2) and helps the positioning of cytosine for the nucleophilic attack by the Zn-bound hydroxide. As the reaction progresses further, the hydrogen bond weakens. The occurrence frequency of the hydrogen bond between the carbonyl O of Ser89 and ammonia is only 15%. The weakening of the hydrogen bond helps the release of the newly formed ammonia.

Binding Mode and Free Energy Difference of Ammonia and Uracil. After ammonia and uracil are formed, our ONIOM[8] calculations indicate that uracil has a similar binding mode as the intermediate analogue in the crystal structure. The product complex MD simulations (**6** and **7** in Figure 2) show that uracil forms a hydrogen-bond network that is similar to the other ligand complexes (Table 9). Ammonia stays on the top of uracil with the distance between N and C4 of uracil of about 3.0 Å, and it forms a hydrogen bond with the carboxyl group of Glu64. When ammonia is exchanged with water, water also forms a similar hydrogen bond with Glu64.

TABLE 10: Chemical Mutation Free Energies between Water and Ammonia

	in water		in protein	
direction of mutation	alchemy	restraint[a]	alchemy	restraint[a]
NH_3 to H_2O (kcal/mol)	−2.74	−8.36	−4.32[b]	−8.36
H_2O to NH_3 (kcal/mol)	2.82	8.36	6.41[c]	8.36

[a] A 1 M standard state was used as a reference state for the gas phase of the dummy atom. [b] Result from subunit 1. [c] Result from subunit 2.

As mentioned above, our recent ONIOM calculation indicates that uracil is released with the help of a water molecule inside the active site.[8] To explore the possibility of ammonia−water exchange, the difference in binding free energy between water and ammonia was evaluated (see Table 10). The forward and backward mutations between water and ammonia in water solution show consistent results, with ∼2.8 kcal/mol from water to ammonia and ∼−2.7 kcal/mol from ammonia to water. The mutation between water and ammonia in the protein active site was performed with the same scheme. The forward mutation (water to ammonia), which was carried out in the active site of subunit 2, gave ∼6.4 kcal/mol, while the backward mutation, which was performed in the active site of subunit 1, gave ∼−4.3 kcal/mol. This indicates that the free energy of chemical mutation is quite sensitive to the environment. The removal of the dummy atom (see Methods section) costs the same free energy as that in water solution, which indicates that this contribution is not sensitive to the environment.

The (average) binding free energy difference between water and ammonia therefore is ∼−2.6 kcal/mol, which shows that water is a better ligand than ammonia. And considering that the reaction takes place in water, the water concentration is much higher than that of the product, ammonia, which makes water movement into the active site easier. Thus, we may conclude that, after the formation of ammonia, it is highly probable that ammonia exchanges with water in the active site.

IV. Concluding Remarks

The MD simulations of yCD in the free form and in complex with its reactant (cytosine), product (uracil), several reaction intermediates, and an intermediate analogue performed in this work provide insights into the reaction mechanism and structural requirements of the enzyme. Quantum chemical calculations to obtain appropriate charges for the simulations around the enzyme active site were carried out, because the presence of the Zn ion and its ligands leads to large electronic structure effects that are reflected in the MD force-field parameterization. For the free enzyme and intermediate analogue complex, the agreements between the simulation results and the X-ray structures are excellent, showing the importance of proper force-field parameterization when metals are ligated with residues whose protonation states are dependent on the metal and the nature and number of ligands.

The simulations of the free enzyme and its intermediate analogue complex show that the protein N-terminus is quite flexible, while all other parts of the enzyme are quite rigid on the MD time scale. The crystallographic data for the free and the intermediate analogue complex forms are very similar,

raising the issue of how substrate enters and product leaves the active site. We do find that the Phe114 loop region and the C-terminal helix sample different configurations in the two subunits, even though the RMSFs for the CA atoms are almost the same and only around 1 Å. This may correspond to a more-or-less rigid body motion of these regions that could permit entrance of a substrate. The 2-ns trajectories may not be long enough to provide enough sampling time to reveal the larger motions that may be required for substrate entry.

Rotation of the carboxyl group of Glu64 is critical to position it relative to the cytosine Zn(HOH/OH) complex and its intermediates to facilitate the various proton transfer steps along the reaction pathway. The MD potential of mean force calculation for Glu64 carboxylate rotation suggests that such motion is feasible on a nanosecond time scale. The MD simulations of the reactant and a series of intermediates also reveal that cytosine adjusts its orientation and position to assist in the nucleophilic attack by the Zn(OH). With reference to Figure 2, the steps along the reaction pathway can be summarized as follows: First, cytosine and yCD form an initial complex (**1** in Figure 2) with cytosine having an orientation rather different from that of the intermediate analogue found in the crystal structures. Second, the binding of cytosine facilitates proton transfer from $Zn(H_2O)$ to form Glu64H and Zn(OH) (**2** in Figure 2). The carboxylic acid group of Glu64H then rotates so that its OH group forms a hydrogen bond with N3 of cytosine (**2′** in Figure 2). Third, Glu64H then transfer its proton to N3 of cytosine to form the yCD hydroxide/Glu64 cytosine−H complex (**3** in Figure 2). The hydrogen bond between the carbonyl oxygen of Ser89 and the amino group of cytosine is strongest at this stage and helps position C4 of cytosine for the subsequent nucleophilic attack by Zn(OH). Fourth, after nucleophilic attack to produce intermediate I (**4** in Figure 2), MD shows that Glu64 hydrogen bonds to N3 (and NH_2) and can again rotate to be reprotonated by C4OH to form intermediate II (**5** in Figure 2). Fifth, the MD trajectory of intermediate II leads to Glu64H hydrogen-bonding to N4 and C4O, which implies that Glu64H has rotated again to point to N4, facilitating decomposition of the tetrahedral complex to the product complex (**6** in Figure 2).

In the MD simulation of the product complex, ammonia forms a stable hydrogen bond with Glu64. On the nanosecond time scale, it does not leave the active site. In view of our previous study[8] that proposed a mechanism for the release of uracil that relies on a water molecule replacing ammonia in its active site, a water molecule was exchanged for ammonia (**7** in Figure 2) and in the subsequent MD simulation, this water forms a similar hydrogen bond with Glu64. Our evaluation of the binding free energy difference between water and ammonia shows that the difference is sufficiently small that, when coupled with the much greater water than ammonia concentration in the active-site vicinity, it is likely for ammonia to readily exchange with water.

Acknowledgment. The work is supported in part by the Center for Biological Modeling of Michigan State University and NIH grants (GM58221 to H.Y. and GM47274 to R.I.C.).

References and Notes

(1) Nishiyama, T.; Kawamura, Y.; Kawamoto, K.; Matsumura, H.; Yamamoto, N.; Ito, T.; Ohyama, A.; Katsuragi, T.; Sakai, T. *Cancer Res.* **1985**, *45*, 1753.

(2) Dipiro, J. T.; Talbert, R. L.; Yee, G. C.; Matzke, G. R.; Wells, B. G. *Pharmacology: A Pathophysiologic Approach*, 3rd ed.; Appleton and Lange: Stamford, CT, 1997.

(3) Morris, S. M. *Mutat. Res.* **1993**, *297*, 39.

(4) Ireton, G. C.; Black, M. E.; Stoddard, B. L. *Structure* **2003**, *11*, 961.

(5) Ko, T. P.; Lin, J. J.; Hu, C. Y.; Hsu, Y. H.; Wang, A. H. J.; Liaw, S. H. *J. Biol. Chem.* **2003**, *278*, 19111.

(6) Xiang, S. B.; Short, S. A.; Wolfenden, R.; Carter, C. W. *Biochemistry* **1995**, *34*, 4516.

(7) Xiang, S. B.; Short, S. A.; Wolfenden, R.; Carter, C. W. *Biochemistry* **1997**, *36*, 4768.

(8) Sklenak, S.; Yao, L.; Cukier, R. I.; Yan, H. *J. Am. Chem. Soc.* **2004**, *126*, 14879.

(9) Dudev, T.; Lim, C. *J. Phys. Chem. B* **2001**, *105*, 10709.

(10) Dudev, T.; Lim, C. *J. Am. Chem. Soc.* **2002**, *124*, 6759.

(11) Simonson, T.; Calimet, N. *Proteins* **2002**, *49*, 37.

(12) Banci, L. *Curr. Opin. Chem. Biol.* **2003**, *7*, 143.

(13) Hoops, S. C.; Anderson, K. W.; Merz, K. M. *J. Am. Chem. Soc.* **1991**, *113*, 8262.

(14) Suarez, D.; Merz, K. M. *J. Am. Chem. Soc.* **2001**, *123*, 3759.

(15) Pearlman, D. A.; Case, D. A.; Caldwell, J. W.; Ross, W. S.; Cheatham, T. E.; Debolt, S.; Ferguson, D.; Seibel, G.; Kollman, P. *Comput. Phys. Commun.* **1995**, *91*, 1.

(16) Case, D. A.; Pearlman, D. A.; Caldwell, J. W.; Cheatham, T. E., III; Wang, J.; Ross, W. S.; Simmerling, C. L.; Darden, T. A.; Merz, K. M.; Stanton, R. V.; Cheng, A. L.; Vincent, J. J.; Crowley, M.; Tsue, V.; Gohlke, H.; Radmer, R.; Duan, Y.; Pitera, J.; Massova, I.; Seibel, G. L.; Singh, C.; Weiner, P.; Kollman, P. A. *AMBER*, v. 7.0; University of California: San Francisco, 2002.

(17) Diaz, N.; Suarez, D.; Merz, K. M. M. *J. Am. Chem. Soc.* **2000**, *122*, 4197.

(18) Cornell, W. D.; Cieplak, P.; Bayly, C. I.; Gould, I. R.; Merz, K. M.; Ferguson, D. M.; Spellmeyer, D. C.; Fox, T.; Caldwell, J. W.; Kollman, P. A. *J. Am. Chem. Soc.* **1996**, *118*, 2309.

(19) Ryckaert, J. P.; Ciccotti, G.; Berendsen, H. J. C. *J. Comput. Phys.* **1977**, *23*, 327.

(20) Essmann, U.; Perera, L.; Berkowitz, M. L.; Darden, T.; Lee, H.; Pedersen, G. L. *J. Chem. Phys.* **1995**, *103*, 8577.

(21) Berendsen, H. H. C.; Postma, J. P. M.; Gunsteren, W. F.; DiNola, A.; Haak, J. R. *J. Chem. Phys.* **1984**, *81*, 3684.

(22) Torrie, G. M.; Valleau, J. P. *Chem. Phys. Lett.* **1974**, *28*, 578.

(23) Frenkel, D.; Smit, B. *Understanding Molecular Simulation: from algorithms to applications*; Academic Press: San Diego, 1996.

(24) Souaille, M.; Roux, B. *Comput. Phys. Commun.* **2001**, *135*, 40.

(25) Boresch, S.; Tettinger, F.; Leitgeb, M.; Karplus, M. *J. Phys. Chem. B* **2003**, *107*, 9535.

(26) Kraulis, P. J. *J. Appl. Crystallogr.* **1991**, *24*, 946.

(27) Bacon, D. J.; Anderson, W. F. *J. Mol. Graphics* **1988**, *6*, 219.

(28) Merritt, E. A.; Bacon, D. J. *Methods Enzymol.* **1997**, *277*, 505.